

# CEBAF Program Advisory Committee Six (PAC6) Proposal Cover Sheet

This proposal must be received by close of business on April 5, 1993 at:

CEBAF  
User Liaison Office  
12000 Jefferson Avenue  
Newport News, VA 23606

## Proposal Title

SEARCH FOR  $\Delta^{++}$  (1232) COMPONENTS IN THE  ${}^3\text{He}$  GROUND STATE

## Contact Person

Name: H. BAGHAEI

Institution: UNIV. OF VA.

Address: CHARLOTTESVILLE, VA 22901

Address:

City, State ZIP/Country: USA

Phone: (804) 924-1781

FAX: (804) 924-4576

E-Mail → BITnet:

Internet:

If this proposal is based on a previously submitted proposal or letter-of-intent, give the number, title and date:

## CEBAF Use Only

Receipt Date: 4/5/93

Log Number Assigned: PR 93-029

By: gp

April 5, 1993

Proposal to the CEBAF PAC6

**Search for  $\Delta^{++}(1232)$  Components in the  $^3\text{He}$  Ground State**

H. Baghaei (co-spokesman), R. A. Lindgren, R. W. Lourie, B. Gladyshev,  
R. Sealock, C. Smith, S. Thornton, and S. Van Verst

*University of Virginia, Charlottesville, VA*

F. W. Hersman (co-spokesman), J. Calarco, T. Smith, I. The, J. Distelbrink

*University of New Hampshire, Durnham, NH*

V. Burkert, M. D. Mestayer, and E. S. Smith

*CEBAF, Newport News, VA*

L. C. Dennis

*Florida State University, Tallahassee, FL*

R. A. Miskimen

*University of Massachusetts, Amherst, MA*

J. M. Laget

*Saclay*

The HALL B Collaboration

## Abstract

We propose to use the CEBAF Large Acceptance Spectrometer (CLAS) to search for pre-existing  $\Delta^{++}(1232)$ -isobars in the  ${}^3\text{He}$  ground state. Theoretical calculations predict the presence of a small percentage of the  $\Delta$ -isobar components in the ground state wave function of few-body systems. However, the existing experimental results are inconclusive, mainly due to the uncertainties in the evaluation of the background (produced  $\Delta$ ) contributions. We propose to study the triple coincidence  ${}^3\vec{H}e(\vec{e}, e'p\pi^+)$  reaction in order to minimize these background contributions (there is no one-step  $\Delta^{++}$  production). A polarized helium target allows a simultaneous measurement of cross sections and asymmetries. The distribution of the coincidence cross section over the acceptance of the CLAS characterizes the initial momentum distribution, while the asymmetry identifies the longitudinal piece associated with knockout. We request 300 hours of beam time at an energy of 4.0 GeV.

## I. Motivation

During the last two decades, theorists have extensively studied the effects of  $\Delta$ -isobar degrees of freedom on the properties of nuclei especially for few-nucleon systems (e.g., binding energy, magnetic moment, and electromagnetic form factors). These studies show the need for inclusion of the isobar degrees of freedom in the calculations in order to remove the discrepancies between the measured quantities and theoretical predictions in the framework of traditional nuclear theory.<sup>1-10</sup> These degrees of freedom are either explicitly included in the nuclear ground state wave functions<sup>1-5</sup> or included, most commonly, in the effective two-body operators acting on nucleonic wave functions.<sup>6-10</sup> The isobar configuration (IC) contributes predominantly to the region of short range correlations and enhances the high momentum components of the nuclear wave function. Therefore, IC effects are expected to be seen mainly at high momentum transfers. Figs. 1 and 2 show the results of some theoretical calculations for the elastic magnetic form factor of  ${}^2\text{H}$  and  ${}^3\text{He}$  which include contributions of the  $\Delta$ .

The basic idea that virtual isobars may be present in the nucleus originate from the possibility of exciting internal nucleon degrees of freedom during collisions of nucleons inside nuclei. The percentage of the isobar components in the nuclear ground state wave function is expected to be small due to the high isobar excitation energy of several hundreds of MeV. According to the theoretical predictions the admixture probability of the  $\Delta\Delta$  component in the  ${}^2\text{H}$  nucleus,  $P_{\Delta\Delta}$ , is at the level of 0.5%<sup>11</sup> and the admixture probability of the  $NN\Delta$  component,  $P_{\Delta}$ , in the nuclei  ${}^3\text{H}$  and  ${}^3\text{He}$  is at the level of 2.5%.<sup>2,4</sup> The probability of  $\Delta$ 's in heavier nuclei could be as high as 7%.<sup>12</sup>

The present evidence in support of the idea of the  $\Delta$  in the nucleus, which mainly comes from measurements of electromagnetic effects at high  $q$ , is indirect although suggestive. Because  $\Delta$ 's play a vital role in all aspects of nuclear structure and

reactions at intermediate energies, it is important to demonstrate the existence of the IC more directly. This can be done by detecting the pre-existing  $\Delta$  in reactions where it either acts as a spectator or is knocked out of the nucleus. However, the smallness of  $P_{\Delta}$  and the presence of other reaction mechanisms (background) which could simulate a final isobar without involving an initial isobar in the nucleus, make the direct study of the pre-existing  $\Delta$  in the nucleus very difficult. In addition, the large nucleon-isobar mass difference that has to be provided to convert a  $\Delta$  which is far off its mass shell to an on mass shell  $\Delta$  along with requiring high energy particles in the final state to reduce final state interactions necessitate high energy projectiles which tends to reduce the counting rates.

So far, the main experimental efforts on direct detection of  $\Delta$ 's in nuclei have been devoted to the search for the  $\Delta\Delta$  configuration in the deuteron (a  $N\Delta$  component is forbidden by deuteron isospin).<sup>13-19</sup> These measurements have been performed with various probes by searching for emission of slow spectator  $\Delta$ 's at backward angles where the background contributions should be reduced. When the spectator  $\Delta$  recoils in the backward hemisphere in the laboratory system, it is less likely to have been produced in the reaction. For example, for a deuteron in a  $\Delta^{++}\Delta^{-}$  bound state, the presence of  $n\pi^{-}$  and  $p\pi^{+}$  combinations simultaneously in the  $\Delta$  mass region with the  $p\pi^{+}$  combination backward in the laboratory frame has been considered to be a signature of the pre-existing  $\Delta$ 's. However, the smallness of the true signal, the difficulties of the experiments (detecting several particles in the final state), and uncertainties in the evaluation of the contribution of background reactions have lead to large uncertainties and variations in the results:  $p_{\Delta\Delta} < 0.2\%-3\%$ . The best upper limit at the present time is, from a more recent  $\nu d$  experiment,  $p_{\Delta\Delta} < 0.4\%$  at the 90% confidence level.<sup>19</sup>

Although the two-nucleon system has been studied most often,  ${}^3\text{He}$  is probably a better nucleus for IC study for several reasons: (1) For  ${}^3\text{He}$ , the isobar configuration has a probability that is larger than the probability predicted for the  $\Delta\Delta$  in the

deuteron. (2) It is possible to have isobar configurations of the form  $NN\Delta$  which is not possible in the  $T=0$  deuteron. Such configurations have an excitation energy of about 300 MeV which is much lower than about 600 MeV for  $\Delta\Delta$  in  ${}^2H$ . Because this low lying state is well separated in energy from the next isobar configuration, it becomes possible to give a cleaner description of the isobars in  ${}^3He$ . (3) There is no  $\Delta^-$  component in  ${}^3He$ . Therefore, its presence in the final state gives a measure of the background contribution. It is to be noted that the three-body system is completely calculable in a nonrelativistic approximation.

There have been a couple of experiments in the 1970's to look for  $\Delta$ 's in  ${}^3He$  and  ${}^4He$ .<sup>20-21</sup> Tatischeff *et al.* studied the  ${}^3He(p,t)\Delta^{++}$  reaction at the incident energy of 850 MeV to search for evidence of  $\Delta^{++}$  components in the  ${}^3He$  wave function.<sup>20</sup> Fig. 3(a) shows different first-order processes that contribute to this reaction. Fig. 3(b) shows the measured missing mass distributions of the  ${}^3He(p,t)X$  reaction for three different triton angles ( $6^\circ$ ,  $10^\circ$  and  $15^\circ$ ). A bump at a mass  $M=1226 \pm 60$  MeV close to that of the free  $\Delta$  is evident which decreases with increasing angle. This measurement did not produce any conclusive results for pre-existing  $\Delta$ 's due to uncertainties in evaluation of the background contributions.

Recently, Lipkin and Lee renewed interest in the search for pre-existing  $\Delta$ 's in  ${}^3He$ .<sup>22</sup> They have demonstrated that the measurement of the  $\pi^+/\pi^-$  ratio in  $(e,e'\pi)$  coincidence experiments provides a sensitive test of  $\Delta$  components in the ground state of  ${}^3He$ . They predict that under certain kinematical conditions the preexisting  $\Delta$  could lead to a large enhancement in the  $\pi^+/\pi^-$  ratio compared to that expected for electroproduction of the  $\Delta$ 's. Their predictions are based on three assumptions: (1) The  $\Delta$  is an object with spin  $3/2$ . (2) Isospin is conserved in the strong interaction which mixes a  $\Delta$  into a nuclear wave function. (3) The amplitude for the absorption of a photon by a  $\Delta$  is proportional to the charge of the  $\Delta$ . The last assumption is valid if one considers the  $\Delta$  to be either an elementary object or a composite object whose constituents are in a totally symmetric wave function.

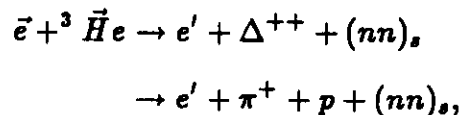
To maximize the sensitivity to the presence of  $\Delta$ 's in the ground state of  ${}^3\text{He}$ , Milner and Donnelly have suggested measuring the ratio of charged pion asymmetries for  $\Delta$ -resonance using a longitudinally polarized electron beam and a polarized  ${}^3\text{He}$  target.<sup>23</sup> The essential point of their discussion is that the spin of the target  ${}^3\text{He}$  nucleus can be used to pick out the longitudinal part of the cross section in the region of the  $\Delta$ . Delta production on the nucleon is predominantly a transverse M1 spin-flip transition with only a relatively small longitudinal C2 piece. However, knockout of a preexisting  $\Delta$  should have no such suppression of the longitudinal response. Based on the same assumptions as Lipkin and Lee, they found that a  $P_{\Delta}=2\%$  could increase the ratio of asymmetries by a factor of two.

Both the Lipkin-Lee and Milner-Donnelly calculations ignore the D-state components, non-resonant contributions, and background due to final state interactions (two-step processes). Since the true signal is expected to be weak, these effects could produce enough background to introduce large uncertainties into any measured  $P_{\Delta}$ . In fact, Laget recently calculated that without detection of the nucleon, any signal from preexisting  $\Delta$ 's is substantially diluted by direct pion production.<sup>24</sup>

A successful experiment should have a signature not easily explained by background processes and the final result should have small model dependence. A very clean way to drastically reduce the background is to observe the  $\Delta^{++}$  in an electron initiated reaction which will automatically eliminate any background due to beam interactions with single nucleons. Furthermore, measurement of this reaction over a significant kinematic range will help differentiate between the quasi-free  $\Delta^{++}$  knock-out, spectator  $\Delta^{++}$ 's emitted after quasi-free elastic scattering on a target neutron or following an interaction with a neutron pair, or two-step processes (which will be addressed later). Finally, measurement of beam-target polarization asymmetries will allow observation of longitudinal-transverse interferences, isolating the longitudinal quasi-free contribution.

This can be accomplished by performing a triple coincidence experiment in which the scattered electron, the proton and the  $\pi^+$  are all detected. CEBAF with its 100% duty cycle and the Large Acceptance Spectrometer (CLAS) is well suited for this kind of measurement. The alkali spin-exchange  $^3\text{He}$  target is well-suited for operation inside the CLAS.

We propose to study quasi-free  $\Delta^{++}$  knockout from the configuration  $\Delta^{++}nn$  in the  $^3\text{He}$  nucleus, via the reaction:



where  $(nn)_s$  denotes a spectator neutron pair. Fig. 4a (4b) shows the diagrammatic representation of the knockout (spectator) process.  $^3\text{He}$  is a favorable nucleus for the investigation, since its large proton excess gives a probability of 50% that a  $\Delta$  present in  $^3\text{He}$  is in the  $\Delta^{++}$  charge state and there is no  $\Delta^-$  component. The  $\Delta NN$  component in  $^3\text{He}$  is predicted to be about 2.4% and the isospin relations give  $\approx 1.2\%$  probability for the  $nn\Delta^{++}$  component.<sup>22</sup>

## II. Count Rate, Background, and Asymmetry Estimates

### Count Rate Estimates

Count rate estimates were made assuming that the cross section for the  $(e,e'\Delta)$  knockout reaction can be treated analogously to the  $(e,e'p)$  reaction. In the plane wave impulse approximation, the  $(e,e'p)$  cross section is given by:

$$\sigma_{ee'p} = K\sigma_{ep}S(p_m, E_m)$$

where  $K$  is a kinematical factor,  $\sigma_{ep}$  is the off-shell ep cross section, and  $S(p_m, E_m)$  is spectral function which represents the joint probability of finding a proton in the nucleus with momentum  $p_m$  and corresponding separation energy  $E_m$ . To

estimate the coincidence cross section for the  $(e,e'\Delta)$  reaction, we first calculated the  $(e,e'p)$  cross section utilizing the Monte Carlo computer program MCEEP<sup>25</sup> and the proton momentum distribution obtained by Jans *et al.*<sup>26</sup> and Marchand *et al.*<sup>27</sup> For example, Fig. 5 shows the calculated  $(e,e'p)$  cross section as a function of the initial momentum for  $E_i = 4$  GeV,  $\theta_e = 15^\circ$ ,  $\omega = 900$  MeV,  $\theta_p = 56^\circ$ , and  $P_p = 1.3$  GeV/c. Then, the  $(e,e'\Delta)$  reaction cross section was estimated from the  $(e,e'p)$  cross section assuming that  $\sigma_{e\Delta^{++}} \approx 4\sigma_{ep}$  and also correcting for the difference between the nucleon and the delta momentum distribution, shown in Fig. 6, according to the calculations of the Hanover group which gives  $P_{\Delta^{++}} \approx 1.2\%$ .<sup>2</sup>

The momentum distribution of nucleons in  $^3\text{He}$  is known from  $^3\text{He}(e,e'p)$  experiments to peak at zero momentum, corresponding to the momentum space wave function of nucleons in  $L=0$  orbital. From spin-isospin considerations, the  $\Delta$  component in the ground state wave function of  $^3\text{He}$  should be in an  $L=2$  orbital with respect to a  $T=1$   $^1S_0$  neutron pair. Fig. 6 shows the Strueve *et al.*<sup>2</sup> calculation of the momentum distribution for the nucleon and the  $\Delta$ -isobar in  $^3\text{He}$ . The peak of the  $\Delta$  momentum distribution is at about 400 MeV/c. Thus, the sensitivity for detecting preexisting isobars can be considerably improved by selecting only  $\Delta$ 's with high initial momentum. The calculations show that a  $^3\text{He}$  component with  $\Delta^{++}$  in an  $L=0$  orbital with respect to a  $^1D_2(nn)$  pair is suppressed.

One of the most basic advantages of CLAS is the ability to map out simultaneously an extensive range of kinematics during a single measurement with one beam energy. Fig. 7 shows the accessible region of  $Q^2 - \omega$  plane for electron scattering off  $^3\text{He}$  at incident energy of 4.0 GeV for one magnet polarity (electrons bend to the axis). The dotted curves show the  $Q^2 - \omega$  values corresponding to the quasielastic scattering and quasifree delta production. Our primary interest is the study of the  $\Delta$  knockout reaction for the  $Q^2 - \omega$  values near the quasifree  $\Delta$  production region. Figs. 8(a)-8(d) show the kinematically allowed range of momentum for the proton, pion, delta and the CLAS acceptance assuming that the residual system (or initial

delta) has a momentum between 150 MeV/c and 700 MeV/c. The acceptance has been calculated for three particles ( $e'p\pi^+$ ) in the final state over the allowed phase space using the FAST Monte Carlo<sup>28</sup> code and reducing the CLAS magnetic field to half of its nominal value to improve acceptance for the low momentum pions.

## Background

As mentioned above, the detection of  $\Delta^{++}$  in the final state eliminates the contribution of the background from quasi-free production. However, two-step processes (final state interactions) can produce backgrounds. Fig. 9 shows diagrammatic representations of the two-step processes in which a produced  $\Delta^+$  undergoes a charge exchange reaction or its decay products undergo a second interaction with another proton in such a way that the final proton and  $\pi^+$  appear to come from the decay of a  $\Delta^{++}$ . There can be similar backgrounds due to processes associated with non-resonant pion production as indicated in Fig. 10. However, the contribution of these reactions are expected to be much smaller than those of Fig. 9 for kinematics near the peak of the delta.

The major background contributions can be eliminated by selecting  $\pi^+p$  events whose invariant mass distribution peaks at the  $\Delta$  mass and that the missing energy of the dineutron is low. The main background which involves two active protons and a charge exchange has a very low probability of producing two low-energy neutrons:<sup>29</sup>

$$e + p + (pn)_s \rightarrow e + \Delta^+ + (pn)_s \rightarrow e + \pi^+ + p + (nn).$$

If the charge exchange occurs after the  $\Delta$  decay into a pion and a nucleon then either one can exchange charge with a spectator nucleon. Moinester and Lipkin have investigated the effects of these two-step processes.<sup>29</sup> They assumed that the backgrounds are proportional to a factor  $P(\text{cx})$  which is the probability of a final

state interaction in which an energetic neutron or  $\pi^0$  interacts with the second proton in  ${}^3\text{He}$ . The neutron ( $\pi^0$ ) must convert to an energetic proton ( $\pi^+$ ) moving in the approximate direction of the original neutron ( $\pi^0$ ), while the recoil neutron should have the appropriate direction and energy to resemble a spectator neutron. For neutron energies around 100 MeV, the back angle elastic scattering (larger than  $160^\circ$ ) will leave a backscattered neutron with less than 20 MeV and also an energetic forward proton. They have made a rough estimate of the effective total charge exchange reaction cross section which gives  $P(\text{cx}) \approx 0.025$ . Therefore, for selected kinematics ( $p_i \approx 200 - 600$  MeV) where the  $\Delta^+$  production is suppressed and the  $\Delta^{++}$  knockout is maximized, the background contribution will be small and the uncertainty associated with their estimates would be minimized.

Fig. 11 shows a calculation of the longitudinal and transverse parts of the cross section for the  ${}^3\text{He}(e,e'\Delta^{++})$  reaction by Laget at  $E_i = 4.0$  GeV,  $\omega = 0.9$  GeV, and  $q = 1.29$  GeV. As can be seen, the contribution of the background to the transverse part is small and the background has no contribution to the longitudinal part.

Background due to multistep processes is the main factor that will limit our ability to determine the size of the  $\Delta$  component of the  ${}^3\text{He}$  ground state. There is no experimental information on these background processes. However, based on the theoretical predictions which place the background at the level of 10-20% of the knockout, we expect to be able to detect the  $\Delta^{++}$  component even if  $P_{\Delta^{++}}$  is as low as 0.2%.

In addition to the above discussed software cuts ( $\pi^+p$  invariant mass around  $\Delta$  mass, and small missing energy) that we will impose on the data to reduce the background contribution, we will also study the following information, which will be available, to further investigate the  $\Delta^{++}$  background: (1) Some information on the background could be obtained by looking for  $\Delta^-$  in the final state. Since there is no  $\Delta^-$  component in  ${}^3\text{He}$  and it cannot be produced from single nucleon, its

presence in the final state must be the result of multi-step processes or uncorrelated production. (2) For small electron scattering angles ( $\approx 15^\circ$ ), we will study the initial momentum distribution of the  $\Delta$  in the nucleus ( $p_i = p_p + p_\pi - q$ , ignoring FSI). At large  $p_i$  ( $>200$  MeV) it is expected to follow the shape of a L=2 pre-existing delta distribution (peak around 400 MeV/c) and at small  $p_i$  ( $<100$  MeV/c) the shape of L=0 distribution of two-step production from nucleons (peak at zero). (3) We will study the yield of the final delta as a function of the electron scattering angle. Since background will be mainly transverse, its contribution will be less important at forward angles.

### Asymmetries

Polarization asymmetries can help to select the longitudinal part of the cross section. The quasi-elastic reaction from pre-existing objects should have a longitudinal dependence characteristic of its charge form factor, and a transverse dependence that maps out the magnetic form factor. Background processes dominated by production followed by final state interactions should be transverse. The dependence of the asymmetry on kinematics would exhibit this behavior.

The cross section for the inclusive scattering of longitudinally polarized electrons off of a polarized spin 1/2 target is:

$$\frac{d\sigma}{d\Omega d\omega} = \Sigma \pm \Delta(\theta^*, \phi^*)$$

where  $\theta^*$  and  $\phi^*$  is the target's spin direction relative to the  $\vec{q}$  vector and the plane of the electron scattering. The  $\pm$  corresponds to the helicity of the incident electron. The spin independent terms are:

$$\Sigma = 4\pi\sigma_M[v_L R_L + v_T R_T]$$

and the spin dependent terms are:

$$\Delta = -4\pi\sigma_M[\cos\theta^* v_{T'} R_{T'} + 2 \sin\theta^* \cos\phi^* v_{TL'} R_{TL'}]$$

where the response functions depend on the invariant electron variables of momentum transfer  $Q^2$  and energy transfer  $\omega$ . If the response functions are written in terms of the form factors of the struck particle, the formulae become:

$$\Sigma = 4\pi\sigma_M[v_L(1+\tau)^2(G_E^\Delta)^2 + 2\tau(1+\tau)v_T(G_M^\Delta)^2]$$

$$\Delta = -4\pi\sigma_M[2\tau(1+\tau)v_{T'}\cos\theta^*(G_M^\Delta)^2 + 2(1+\tau)\sqrt{2\tau(1+\tau)}v_{TL'}\sin\theta^*\cos\phi^*G_M^\Delta G_E^\Delta]$$

where the  $G_E^\Delta$  and  $G_M^\Delta$  in this case represent the electric and magnetic form factor of the  $\Delta^{++}$ . Measuring the asymmetry as a function of  $Q^2$  will exhibit this relationship between charge and current if the reaction process is indeed quasifree knockout.

We have performed an estimate of the precision of this asymmetry measurement. The calculation was performed for a 4 GeV beam with polarization of 75%, and a target polarization of 40% oriented at 130° in the lab. A luminosity of  $L = 3 \times 10^{33}$  electrons-baryons/cm<sup>2</sup>/sec for 300 hours, equally divided between electron helicities, was used. A 1% component of  $\Delta^{++}$  in the <sup>3</sup>He wave function, and a detection efficiency for triple coincidence of 20% was assumed. In Fig. 12 we plot the estimate of the asymmetry and the uncertainty in the asymmetry.

### III. Target and Magnetic Field

The target technology we have selected for this measurement has been developed over the past 8-10 years by Tim Chupp and collaborators,<sup>30</sup> and used in several measurements at several laboratories. The high density offered by this technology permits the maximum CLAS luminosity at low beam currents, as well as reduces greatly the sensitivity of the polarization to magnetic field gradients. Consequently it is the most appropriate and conservative target choice. Integration of this target into the CLAS is nevertheless a complex issue. We discuss below several of our considerations. The target is currently under construction at the University of New Hampshire.

The  $^3\text{He}$  target contains 10 atmospheres of helium, or  $2.7 \times 10^{20}$  atoms/cm<sup>3</sup> over a length of 15 cm, for a total thickness of 20 mg/cm<sup>2</sup> or  $4 \times 10^{21}$  atoms/cm<sup>3</sup>. An equal areal thickness is in each beam window, assumed to be 90  $\mu\text{m}$  Corning 1720 glass. A beam current of 30 nA will provide a luminosity of  $3 \times 10^{33}$  electron-nucleon/cm<sup>2</sup>sec on helium or  $1 \times 10^{34}$  electron-nucleon/cm<sup>2</sup>sec on the entire target. Since the target walls and the holding field magnet provide some shielding of the wire chambers, this luminosity is within CLAS design goals.

The  $^3\text{He}$  target is polarized by optically pumping an alkali metal vapor (rubidium) which spin exchanges with helium. Circularly polarized light of 795 nm can be absorbed by s-shell electrons with the opposite polarization, promoting them to the p-shell. Subsequent collisions with helium and nitrogen mix the p-shell polarization and promote nonradiative decays to the ground state, with equal probability for each spin state. The depletion of one spin state leads to accumulation of rubidium polarization. Polarization is transferred to helium nuclei through the hyperfine interaction during collisions.

The design uses two cells, a pumping cell and a target cell. The pumping cell is maintained at elevated temperature, adjusted to control the rubidium vapor pressure. It is located 5 cm off-axis. It must be fully illuminated to maximize the polarization. The target cell is held at a lower temperature to assure that the rubidium plates out on the transfer capillary. Target polarization is measured by adiabatic fast passage nuclear magnetic resonance.

Coincidence quasielastic scattering from neutrons in 100 torr of nitrogen contributes a 14% dilution over the volume of the cell. Coincidences from scattering in the glass can be eliminated by track reconstruction. Scattering from nitrogen is measured with an equivalent target of the same geometry (with additional nitrogen) and subtracted. We continue to seek ways of reducing the nitrogen and window thicknesses.

## Magnetic fields

A new magnet design is used to define the quantization axis. Two independent coils are wrapped around a watermelon-shaped shell 30 cm diameter and 50 cm long. The first coil of aluminum wire is wound like a solenoid to provide a uniform axial field. A dipolar coil wound in a cosine-theta configuration will provide a uniform field along an axis perpendicular to the beam. By adjusting the current in these two windings, an arbitrary spin quantization direction can be achieved.

While the goal is to immerse the entire target in a single uniform magnetic field, the magnetic field is subject to two distinct constraints. As the helium diffuses throughout the target volume it samples the magnetic field in different regions. Spatial variations of the field appear locally to a moving helium atom as time variations, leading to spin relaxation. The relaxation rate is half the diffusion velocity ( $D=0.5 \text{ cm}^2/\text{sec}$ ) multiplied by the fractional change in magnetic field per unit length.

$$\Gamma_B = \frac{1}{2} D \frac{(\nabla B_T)^2}{B_0^2}$$

A uniformity of one half percent per centimeter is required to contribute less than 50 hours to the relaxation time ( $\Gamma_B^{-1}$ ).

The precision of the data, in particular the location of the point of zero asymmetry, can be determined with a precision no greater than the knowledge of the quantization axis. This requires that the magnetic field along the beam be uniform and precisely known. This source of systematic uncertainty will be reduced to 4 mrad with a magnet uniformity of one percent. This is the overall design goal for our holding field magnet.

Each coil will be wound with approximately 0.5 mm aluminum wire. The solenoid will have two wrapping layers, while the cosine-theta coil will be accomplished by varying the number of layers from 1 to 4. The total thickness of the conductors is

approximately 3 mm. A plastic sheath encloses the water cooling jacket. Scattered electrons and ejected particles pass through the glass walls of the target cell and through the aluminum conductors on their path to the region one drift chambers. This additional multiple scattering limits the trajectory reconstruction of low momentum charged particles, but contributes only 2 mr to electrons at 1 GeV/c. The influence on momentum reconstruction is minimal.

The target will have the capability of polarization measurement and fast spin flip by adiabatic fast passage nuclear magnetic resonance. The primary field is provided by the coils in the watermelon magnet. We intend to include the drive coils in the watermelon magnet as well. Their winding configuration is identical to the primary winding, a solenoid and a cosine-theta coil, providing fields in the same plane (also containing the beam). If they are driven in phase and adjusted at the correct proportion, they produce an oscillating field perpendicular to the primary field. The pickup coils will be small Helmholtz windings located against the pumping cell, and perpendicular to the plane containing the beam and the spin direction. (Note that a conventional drive coil could also be used, with the drawback that it fixes the target angle.)

This new watermelon magnet does not physically interfere with using the normal configuration of the CLAS mini-toroid and region one drift chamber as shown in Fig. 13. (Note that the conventional CLAS first and second level triggers, as well as the standard acquisition and analysis software can also be used without modification.) However careful attention must be paid to the minitoroid's magnetic field. The minitoroid sweeps Møller electrons from the wire chamber with approximately 200 kA-turns producing 0.1 Tesla fields. These fields leak into the target region leading to off-axis fields that increase as the fifth power of the radius. While these contributions would not effect the precision of the field at the beam axis, they would reduce the relaxation time. The field  $B_\phi$  reaches 2 gauss at 5 cm, the location of the pumping cell, and rises to 20 gauss at 8 cm (for a particular coil shape). In-

creasing the inner diameter of the minitoroid a factor of two (from 17 cm to 34 cm) would reduce these fields by a factor of 32, but eliminate the effectiveness of the Møller sweeping. Instead, the outer windings of the minitoroid can be used for the sweeping field, and the innermost winding be used to contain the leakage fields and cancel the gradients. Approximately 10% of the total current flowing in the opposite direction on the inner winding cancels the gradients (Fig. 14). To achieve the design magnetic field uniformity, this cancellation must be accomplished with an accuracy of 10%. By shimming the spacing between the main loops and the canceling loop the cancellation can be exact. We intend either to influence the design of the minitoroid, or fabricate one meeting our requirements.

#### IV. Experimental Plan

We plan to use the CEBAF Large Acceptance Spectrometer (CLAS) for polarized  ${}^3\text{He}(e,e'p\pi)$  measurements. The large solid angle and large momentum acceptance of the CLAS make it well suited for study of the triple coincidence experiments. Its relatively low luminosity, which will help to achieve a good signal (true coincidence) to noise (accidental coincidence) ratio, will be compensated by its large acceptances. Its momentum resolution ( $\leq 1\%$ ) will be sufficient for our experiment. The CLAS standard detection apparatus will be used for detecting and identifying particles.

Since the count rate is small, the maximum luminosity that CLAS can handle (about  $10^{34} \text{ cm}^{-2}\text{sec}^{-1}$ ) will be used. The large electron, proton and pion single rates requires that CLAS be triggered on events with a second particle in coincidence with the electron. The CLAS detector system will allow us to make fast trigger decisions using information from the Čerenkov counter, scintillator hodoscope and shower counter.

## References

- [1] R. Dymarz and F.C. Khanna, Phys. Rev. C **41**, 2438 (1990); Nucl. Phys. **A507**, 560 (1991).
- [2] W. Strueve, Ch. Hajduk, P.U. Sauer and W. Theis, Nucl. Phys. **A465**, 651 (1987); Ch. Hajduk, P.U. Sauer and W. Strueve, *ibid.* **A405**, 581 (1983); *ibid.* **a405**, 620 (1983).
- [3] W. Leidemann and H. Arenhovel, Nucl. Phys. **A465**, 573 (1987).
- [4] A. Picklesimer, R.A. Rice, and R. Brandenburg, Phys. Rev. C **44**, 1359 (1991); Phys. Rev. C **45**, 2624 (1992).
- [5] P. G. Bluden, W.R. Grennberg, and E. L. Lomon, Phys. Rev. C **40**, 1541 (1989); W.P. Sitarski, P. G. Bluden, and E. L. Lomon, Phys. Rev. C **36**, 2479 (1987).
- [6] R. Schiavilla, R. B. Wiringa, V. R. Pandhariponde, and J. Carlson. Phys. Rev. C **45**, 2628 (1992).
- [7] R. Schiavilla, and D. O. Riska, Phys. Rev. C **43**, 437 (1991).
- [8] J. Carlson, D. O. Riska, R. Schiavilla, and R. B. Wiringa, Phys. Rev. C **42**, 830 (1990); *ibid.* **44**, 619 (1991).
- [9] E. Hadjimichael, B. Goulard, and R. Bournais, Phys. Rev. C **27**, 831 (1983).
- [10] R. Schiavilla and D. O. Riska, Phys. Rev. C **43**, 437 (1991).
- [11] H. J. Weber and H. Arenhovel, Phys. Rep. **36C**, 277 (1978); A. M. Green, Rep. Prog. Phys. **39**, 1109 (1976)

- [12] M. R. Anastasio *et al.*, Nucl. Phys. **A322**, 369 (1979); R. Cenni, F. Conte, and U. Lorenzini, Phys. Rev. C **39**, 1588 (1989).
- [13] C. P. Horne *et al.*, Phys. Rev. Lett. **33**, 380 (1974).
- [14] H. Braun *et al.*, Phys. Rev. Lett. **33**, 312 (1974).
- [15] M. J. Emms *et al.*, Phys. Lett. **52B**, 110 (1974).
- [16] P. Benz and P. Soding, Phys. Lett. **52B**, 367 (1974).
- [17] B. S. Aladashvili *et al.*, Nucl. Phys. **B89**, 405 (1975).
- [18] R. Beurtey *et al.*, Phys. Lett. **61B**, 409 (1976).
- [19] D. Allasia *et al.*, Phys. Lett. B **174**, 450 (1986).
- [20] B. Tatischeff *et al.*, Phys. Lett. **77B**, 254 (1978).
- [21] B. Badelek *et al.*, Phys. Lett. **81B**, 308 (1979).
- [22] H. J. Lipkin and T.-S. H. Lee, Phys. Lett. B **183**, 22 (1987).
- [23] R. G. Milner and T. W. Donnelly, Phys. Rev. C **37**, 870 (1988).
- [24] J. Laget, private communication.
- [25] P. Ulmer, MCEEP: Monte Carlo for Electro-Nuclear Coincidence Experiments, CEBAF-TN-91.
- [26] E. Jans *et al.*, Phys. Rev. Lett. **49**, 974 (1982).
- [27] C. Marchand *et al.*, Phys. Rev. Lett. **60**, 1703 (1988).

[28] E. Smith, Fast Monte Carlo Program for the CLAS Detector, CLAS-NOTE-90-003.

[29] M. A. Moinester and H. J. Lipkin, Phys. Lett. **B277**, 221 (1992).

[30] T. E. Chupp *et al.*, Phys. Rev. C **45**, 915 (1992).

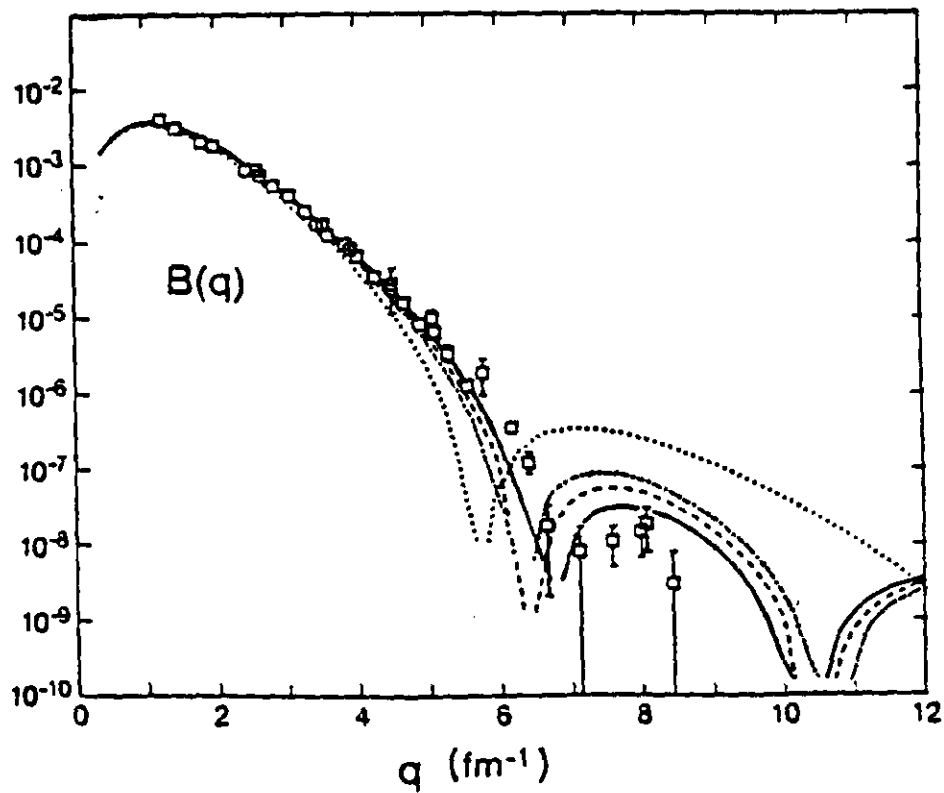


Figure 1. The elastic magnetic form factor data of the deuteron compared to the theoretical calculations of Ref. 1 (assuming  $p_{\Delta\Delta}=0.35\%$ ). Nucleon currents only (dotted curve); nucleon and isobar currents (dash-dotted curve); nucleon and isobar currents plus  $\pi$ -pair MEC (dashed curve). Solid curve is the full calculation that also includes the  $\rho\pi\gamma$ -current contribution (Ref. 1).

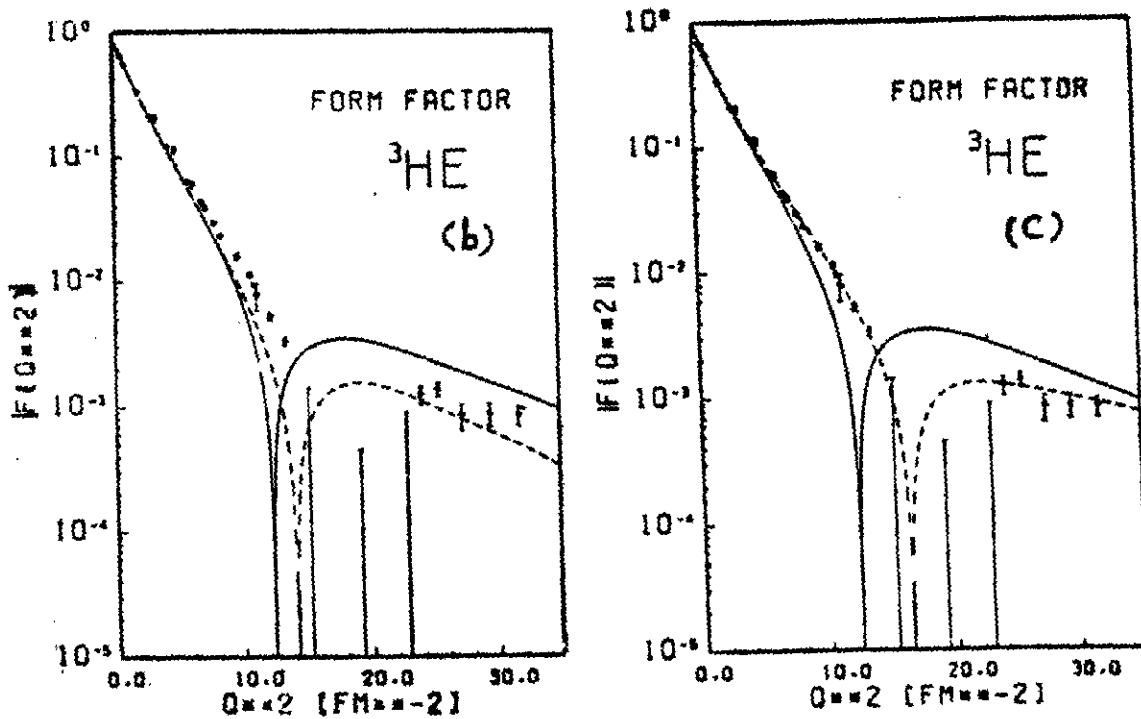
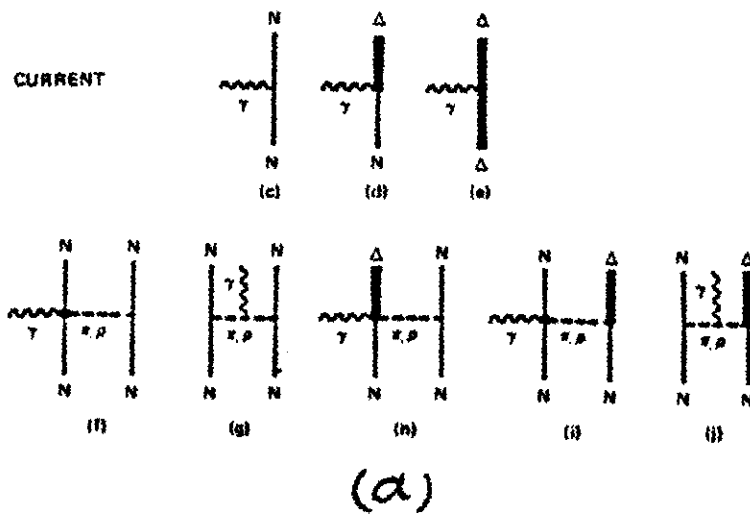


Figure 2. (a) Processes assumed to contribute to the  ${}^3\text{He}$  elastic magnetic form factor, from Ref. 2 (assuming  $p_{\Delta}=2.5\%$ ). (b) The dashed curve shows the purely nucleonic results containing the contributions from the two-nucleon currents of diagram (f) and (g). The solid curve refers to all the current operators. (c) The solid curve is the same as in Fig. (b). The dashed curve is the full calculation including relativistic corrections (Ref. 2).

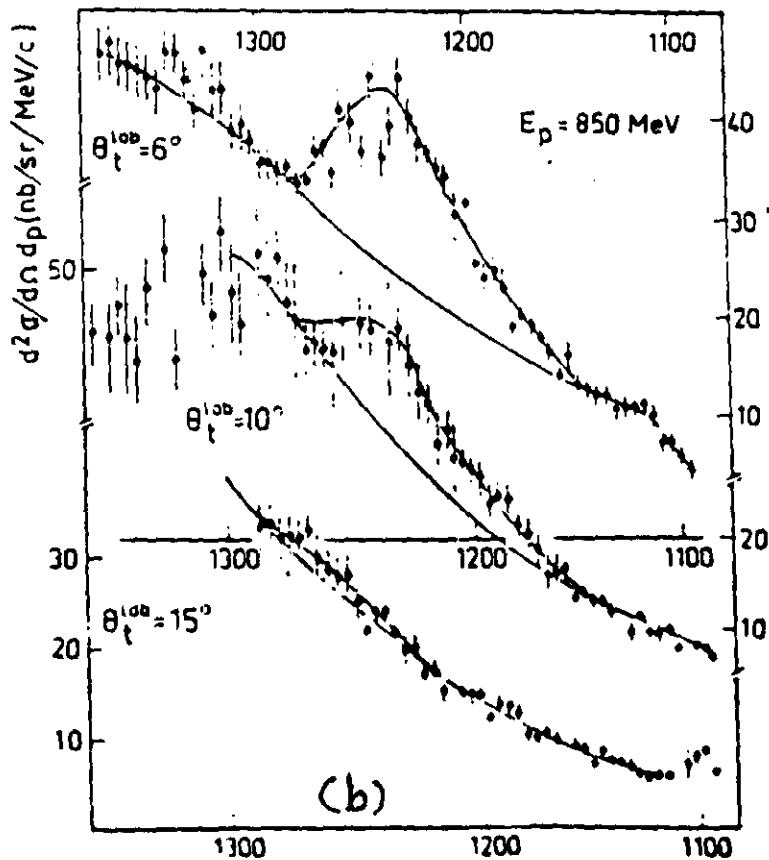
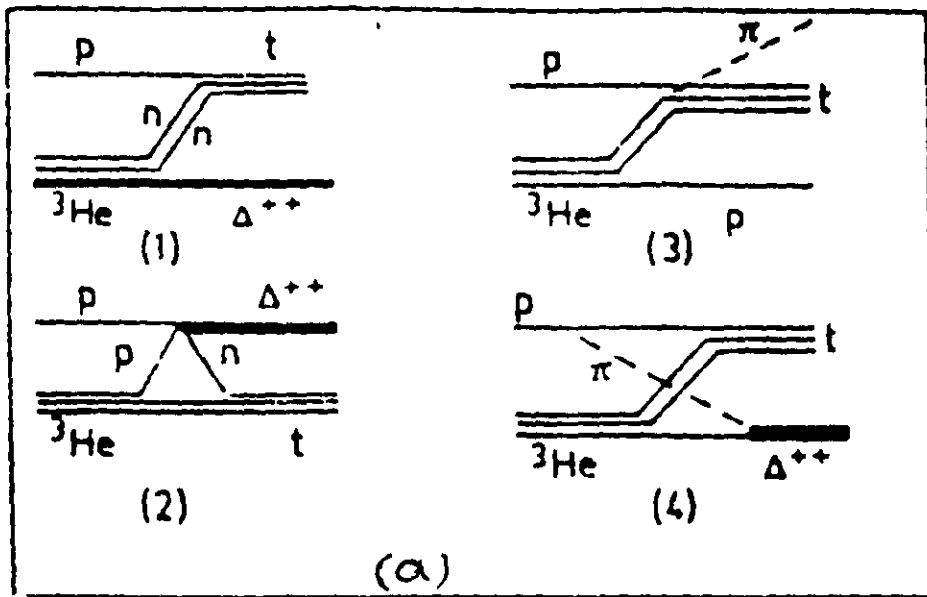


Figure 3. (a) Graphs of different processes that could contribute to the  ${}^3\text{He}(p,t)\Delta^{++}$  reaction. (b) Measured missing mass distribution of the  ${}^3\text{He}(p,t)X$  reaction at  $E_p=800$  MeV (Ref. 21).

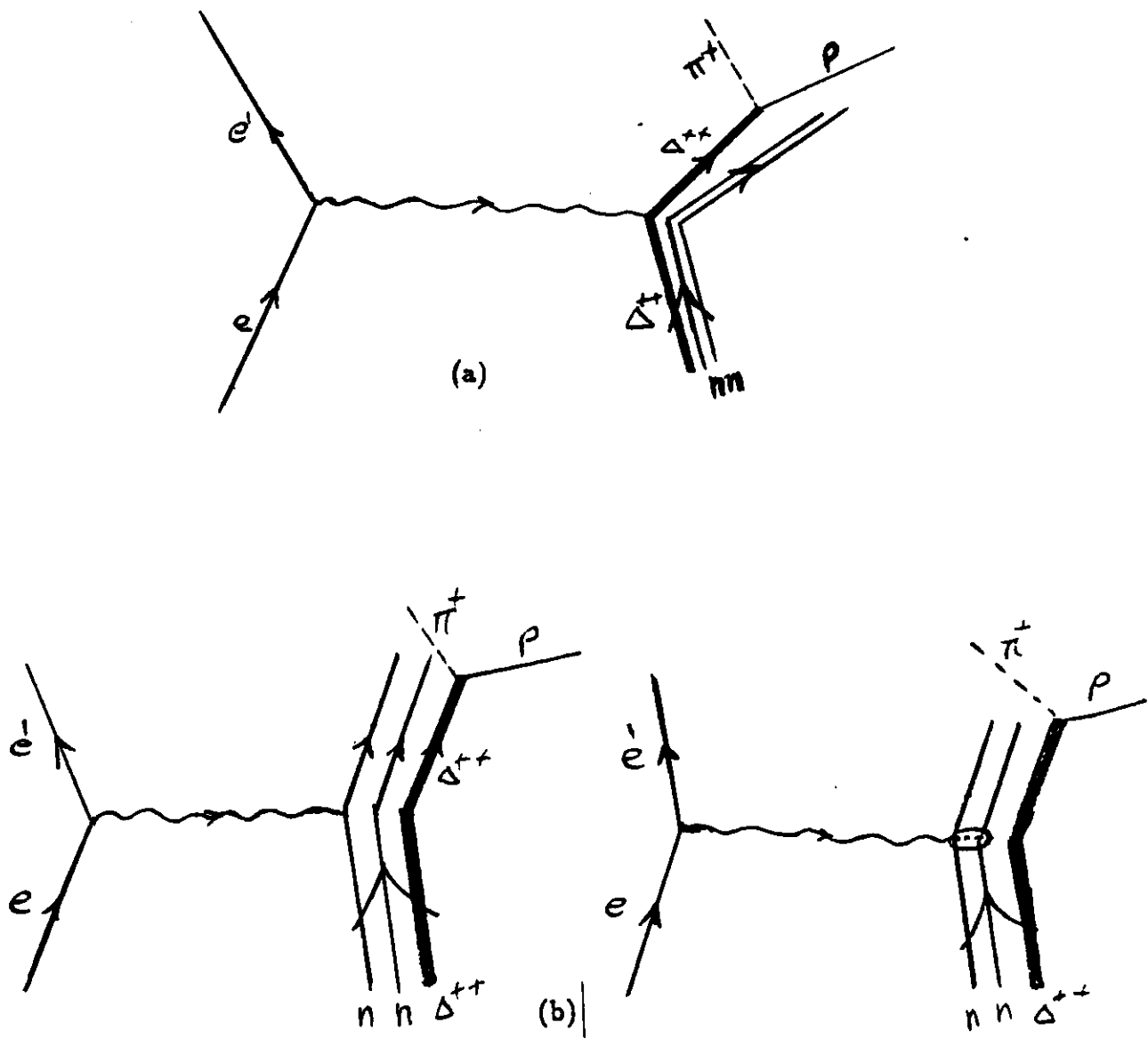


Figure 4. Schematic representation of the (a)  $\Delta^{++}$  knockout reaction, and (b)  $\Delta^{++}$  spectator process.

${}^3\text{He}(e,e'p)$ ,  $E=4.0$  GeV

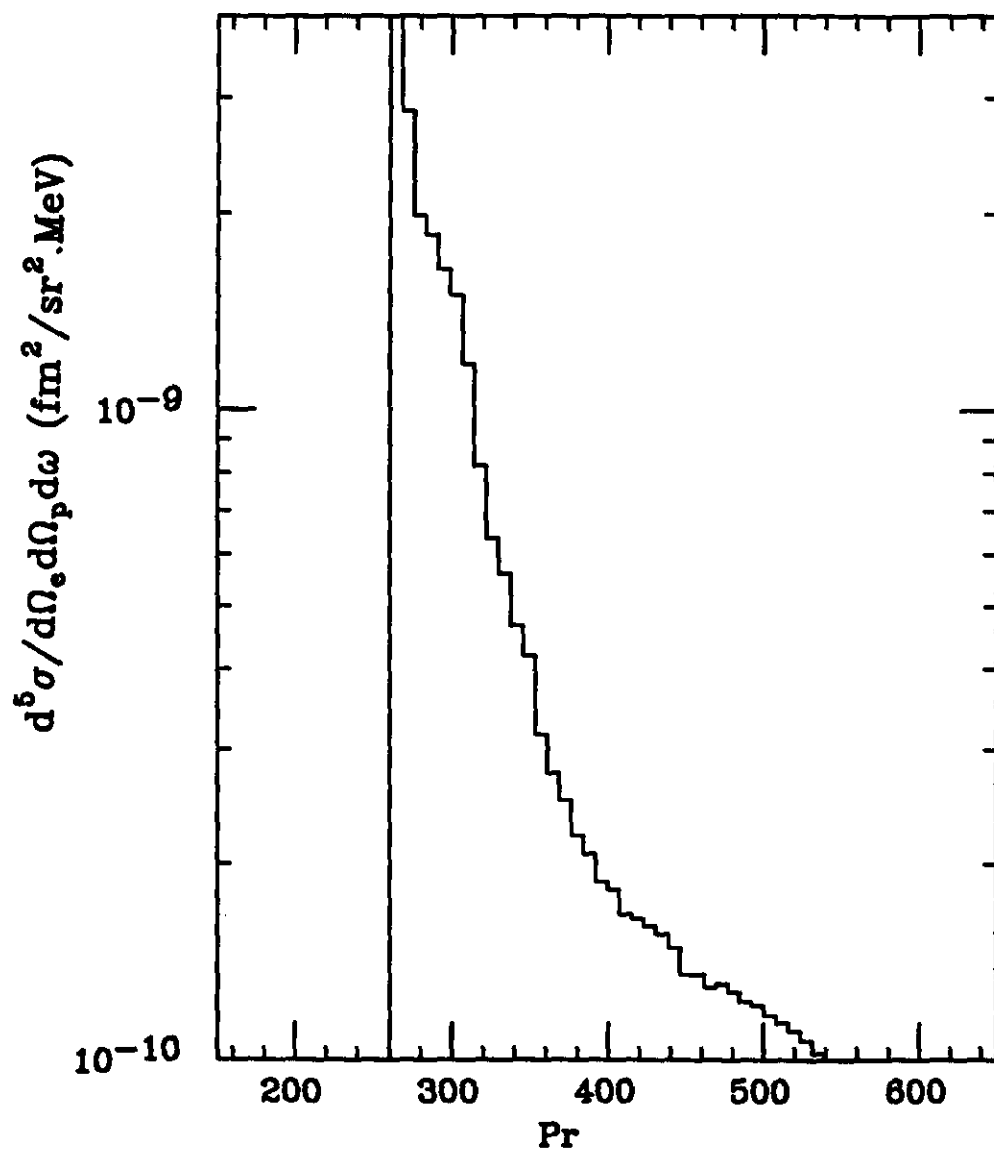


Figure 5. A typical  $(e,e'p)$  cross section as a function of the initial momentum at  $E_i=4$  GeV,  $\theta_e=15^\circ$ ,  $q = 1.3$  GeV/c,  $\theta_p = 56^\circ$ , and  $P_p = 1.3$  GeV/c.

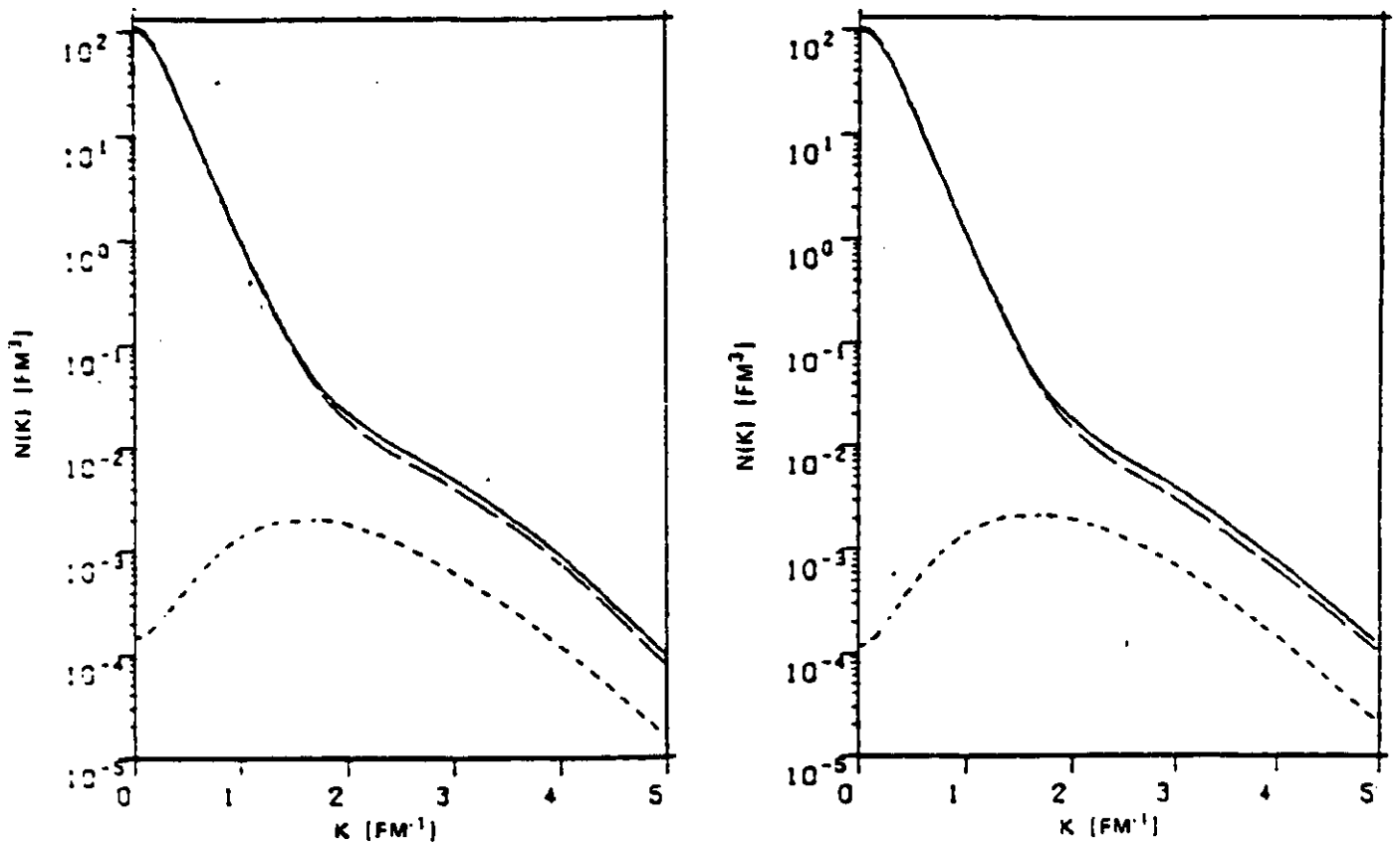


Figure 6. Momentum distributions in the three-nucleon bound state. The nucleonic distribution arising from a calculation with (solid curve) and without (dashed curve)  $\Delta$ -isobar components are shown and compared to the distribution of the  $\Delta$ -isobar (short dashed curve) for two different potentials (Ref. 2).

$e-{}^3\text{He}$ ,  $E=4$  GeV

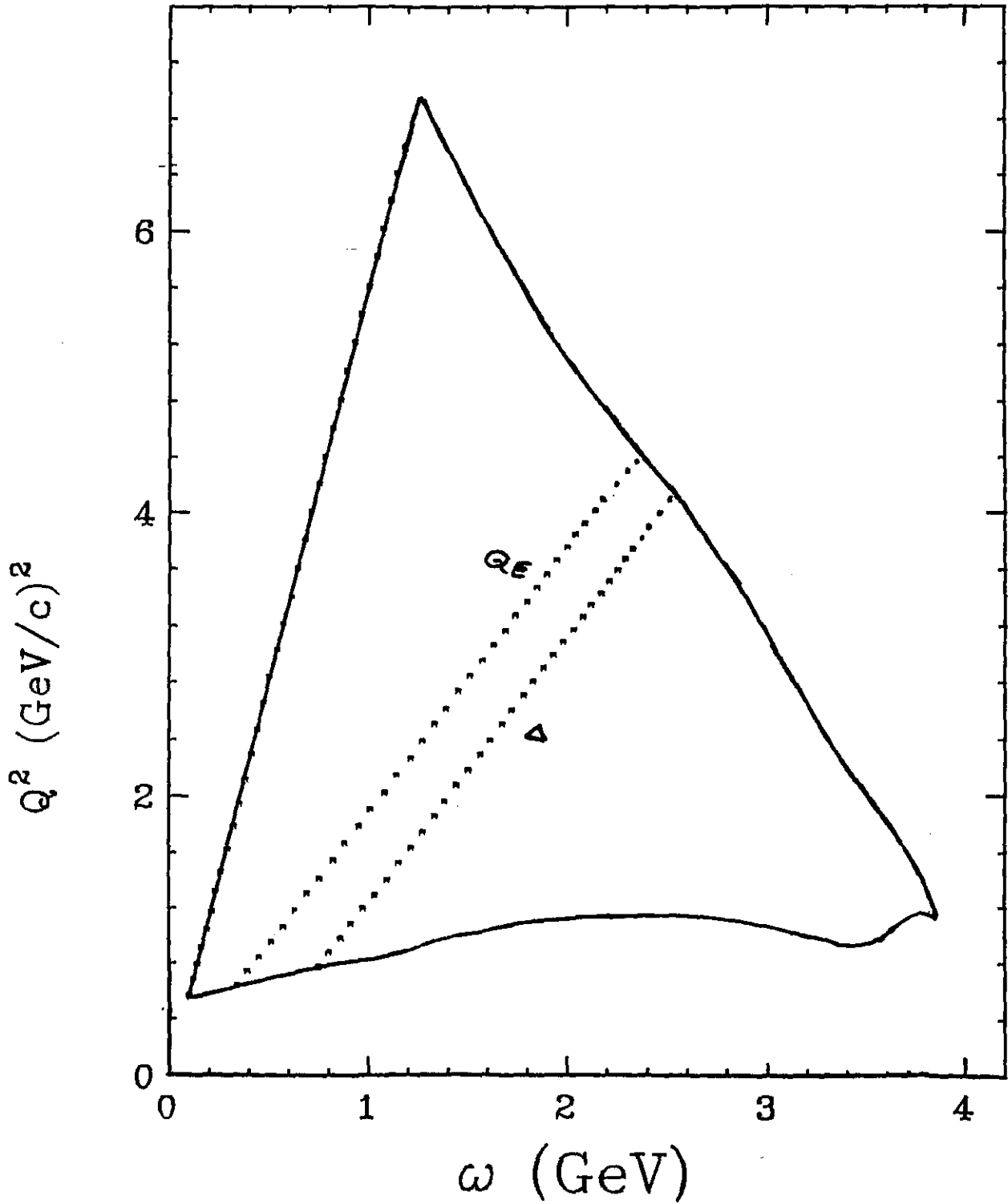


Figure 7. The kinematically allowed region of  $Q^2-\omega$  plane for the electron scattering off a  ${}^3\text{He}$  at  $E_i = 4.0$  GeV. The dotted curves show the  $Q^2-\omega$  corresponding to the quasielastic (QE) and the quasifree delta production peaks.

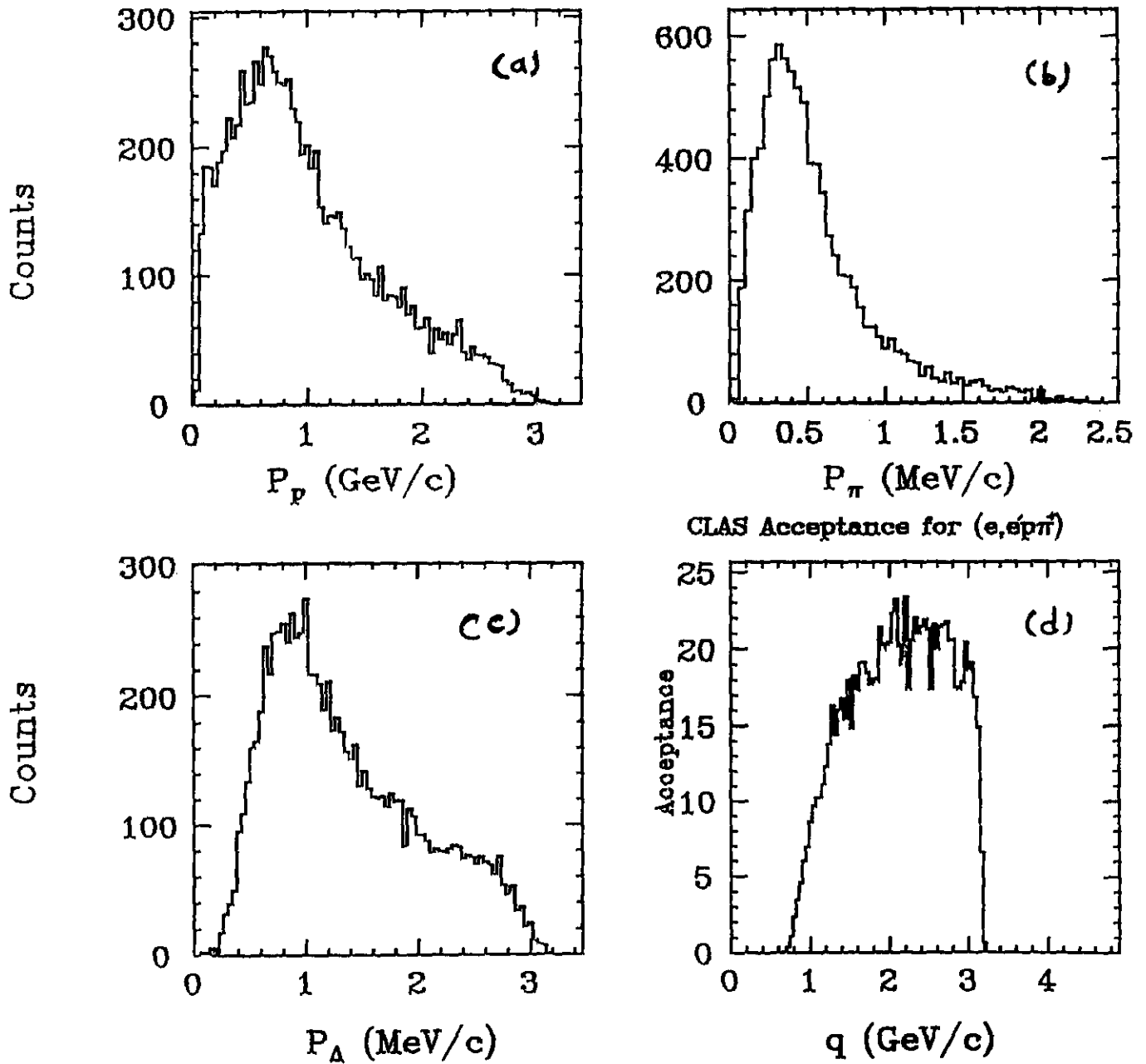


Figure 8. Momentum distribution of the final (a) protons, (b) pions, and (c) delta for  $Q^2 - \omega$  corresponding to the delta region. (d) CLAS acceptance for triple coincidence ( $e'p\pi^+$ ) as a function of momentum transfer.

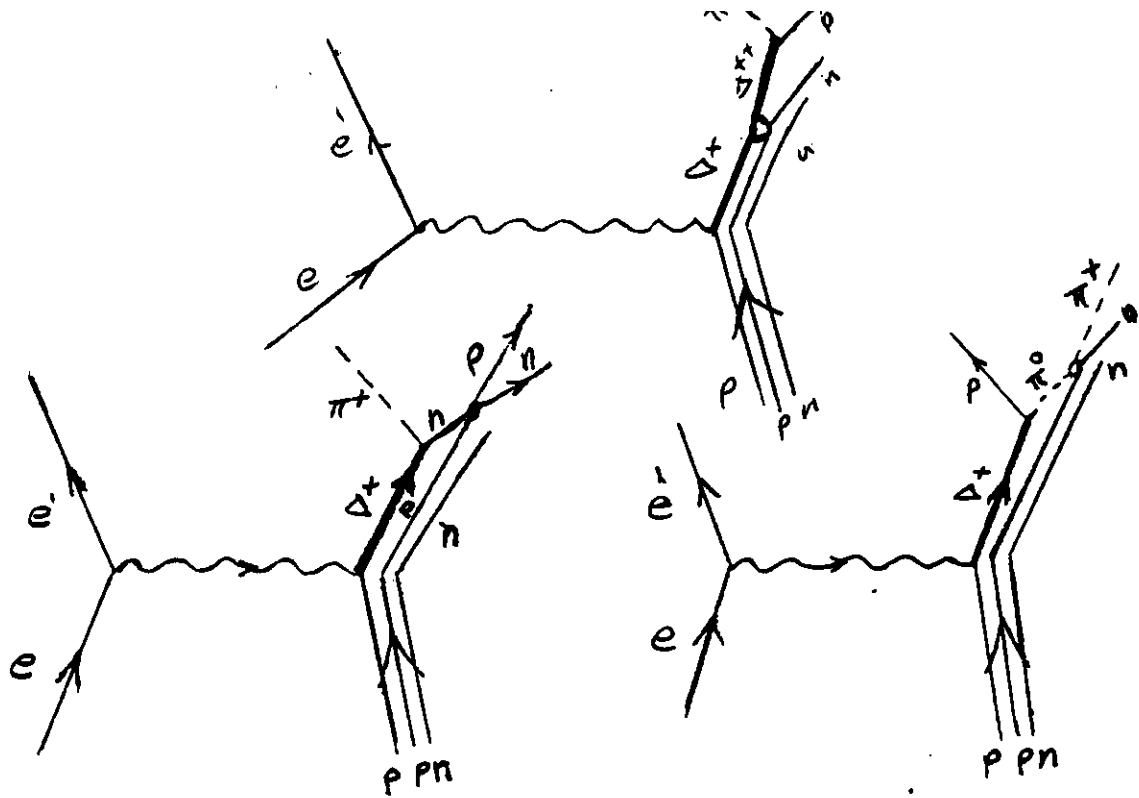


Figure 9. Schematic representation of the resonant two-step background processes.

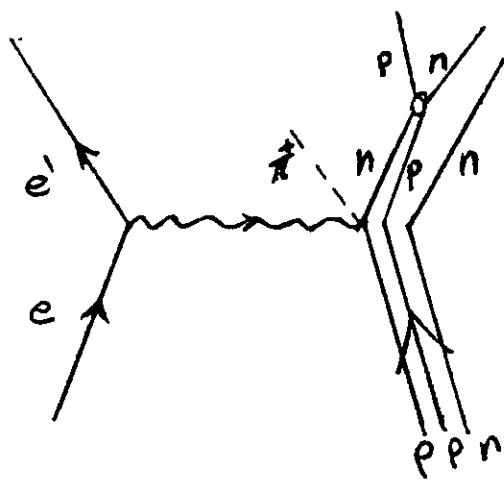


Figure 10. Diagrammatic representation of the nonresonant two-step background processes.

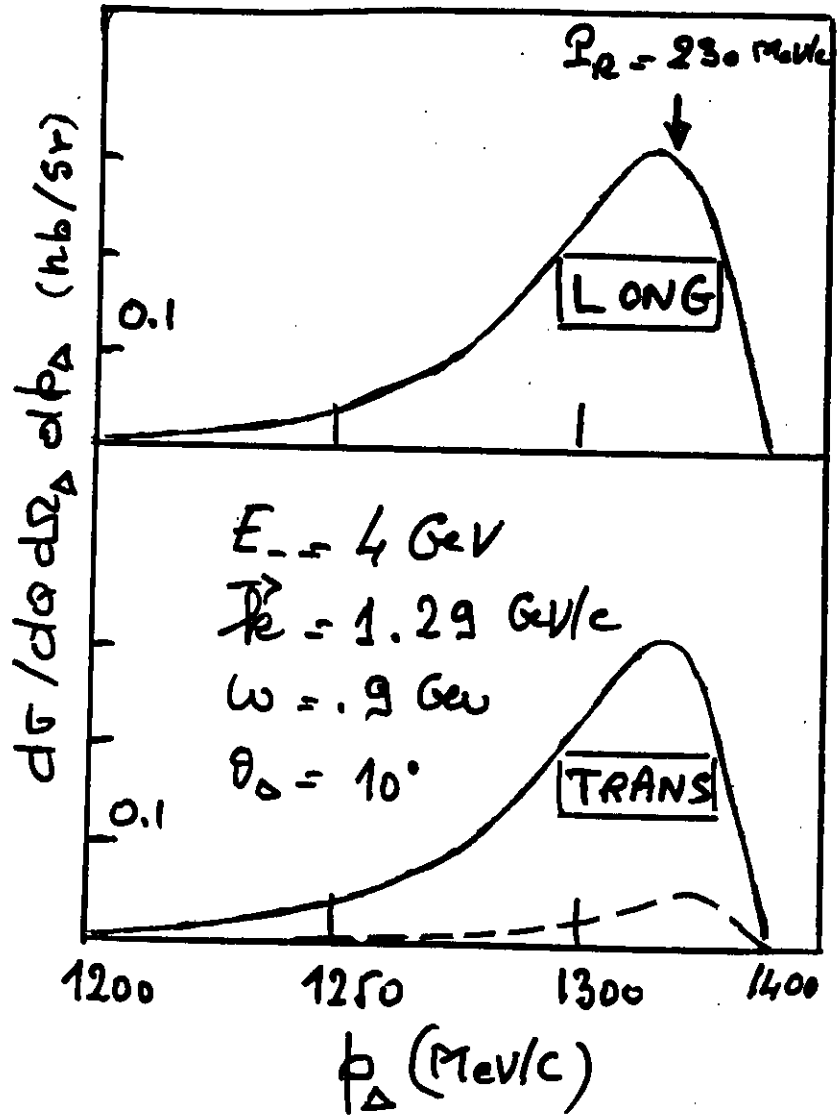


Figure 11. Longitudinal and transverse parts of the cross section for  ${}^3\text{He}(e,e'\Delta^{++})$  reaction at  $E_i = 4.0 \text{ GeV}$ ,  $\omega = 0.9 \text{ GeV}$ , and  $q = 1.29 \text{ GeV}$ . The dashed curve show the background contributions.

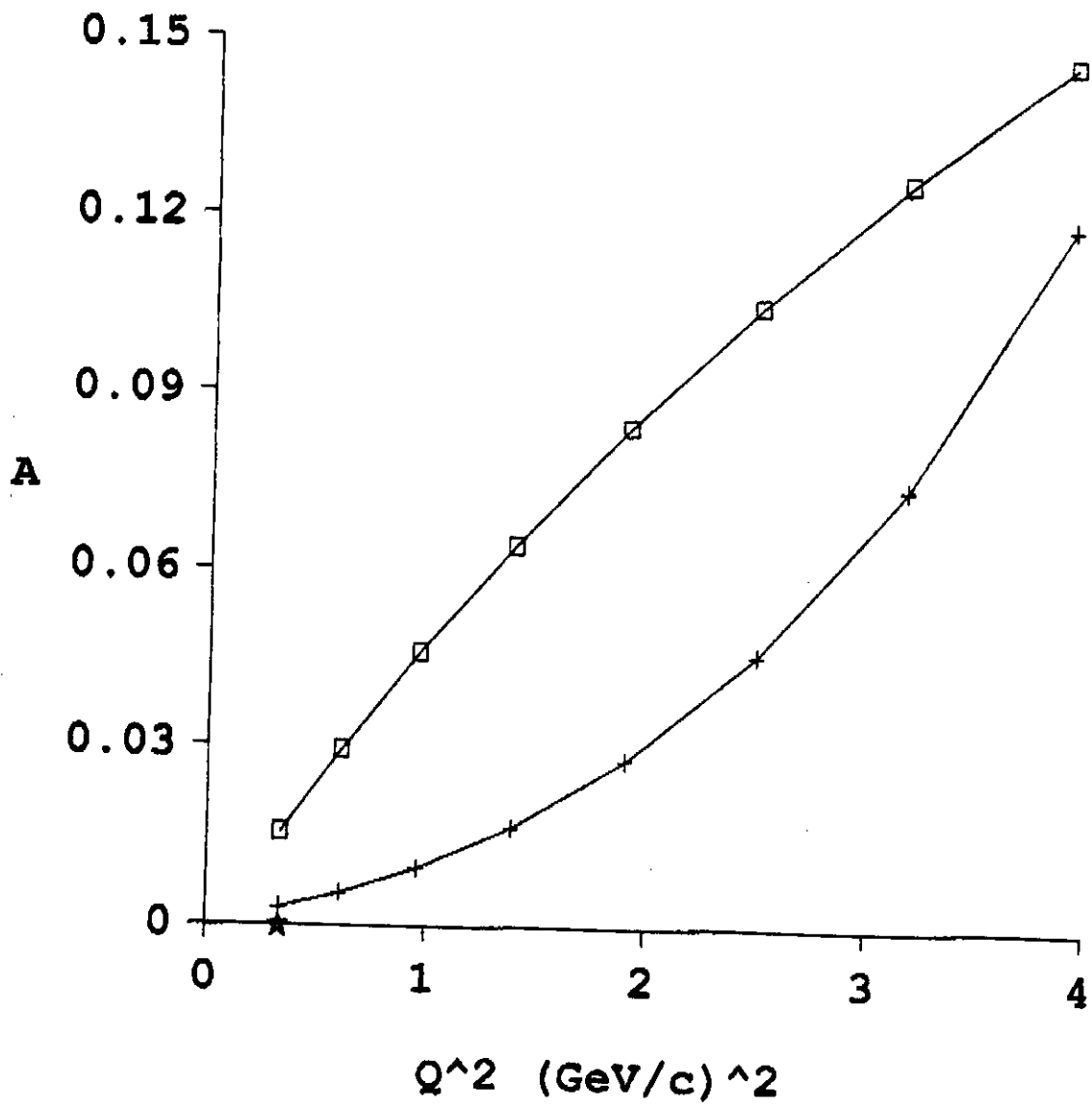


Figure 12. Estimate of the asymmetry (upper curve) and the uncertainty in the asymmetry (lower curve) for the  $\Delta^{++}$  knockout reaction.

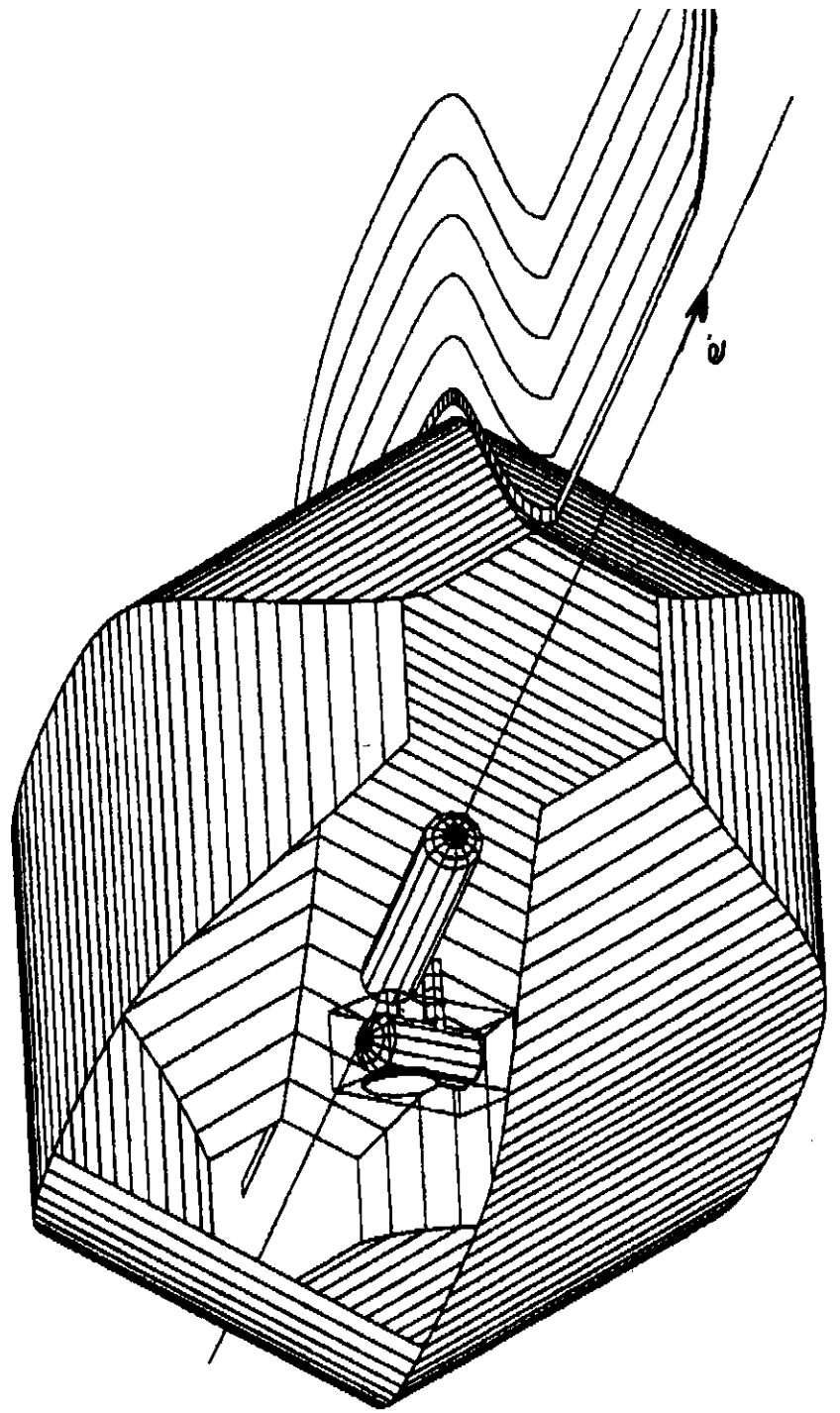


Figure 13. The alkali spin exchange helium target integrated in the CLAS. The minitoroid coil with its gradient canceling loops, the watermelon holding field magnet, and the two-cell target are indicated. Granularity in surfaces of revolution are an artifact of the drawing program.

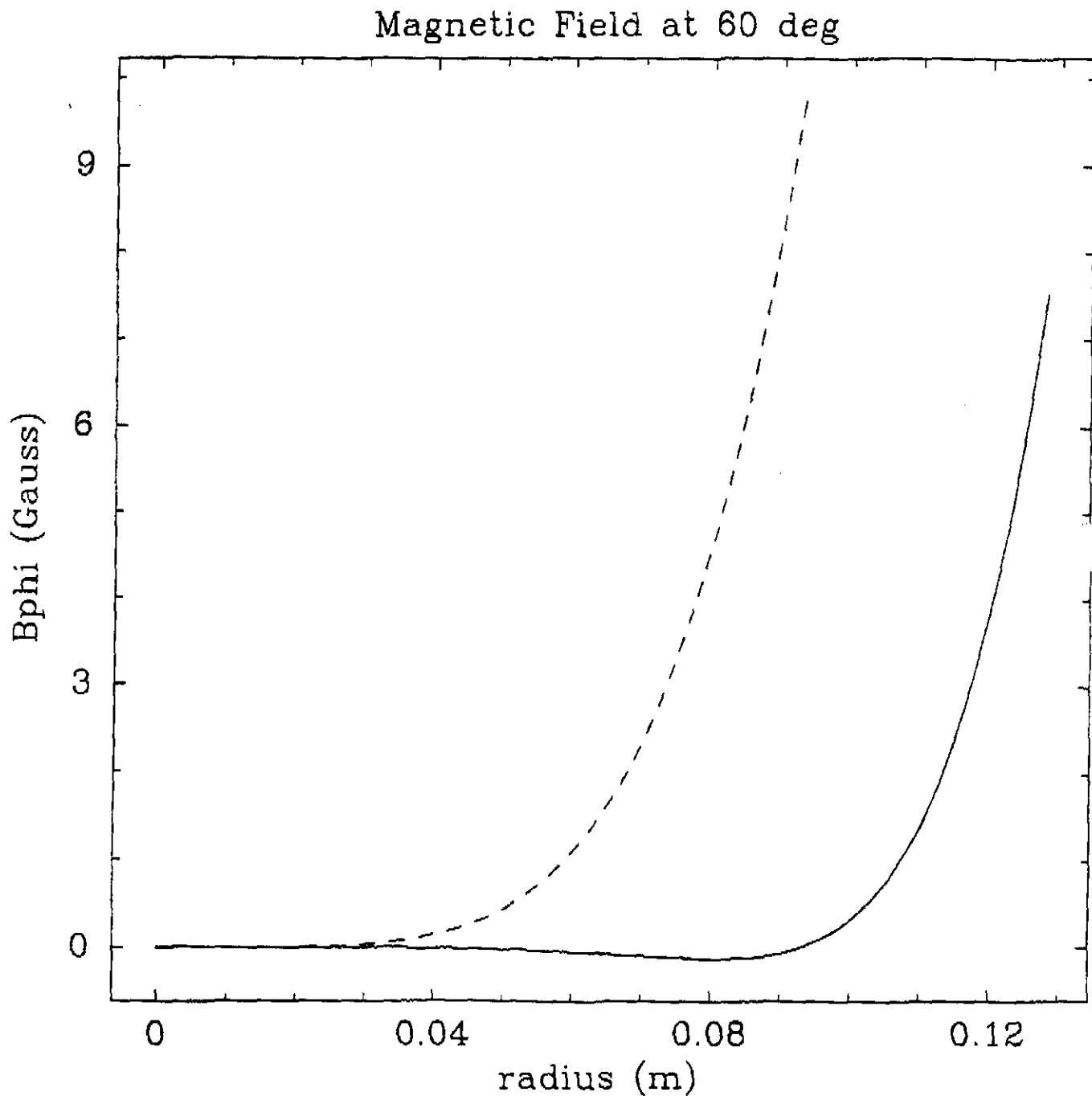


Figure 14. Azimuthal component of magnetic field at the midplane between coils as a function of radius from the nominal target position. Nominal fields rise as the fifth power of the radius. These fields can be canceled by a current in closer proximity flowing in the opposite direction.